Energy 68 (2014) 174–181

Contents lists available at ScienceDirect

Energy

journal homepage: www.elsevier.com/locate/energy

Bypass ejector with an annular cavity in the nozzle wall to increase the entrainment: Experimental and numerical validation

Yinhai Zhu*, Peixue Jiang

Key Laboratory for Thermal Science and Power Engineering of Ministry of Education, Beijing Key Laboratory of CO_2 Utilization and Reduction Technology, Department of Thermal Engineering, Tsinghua University, Beijing 100084, China

ARTICLE INFO

Article history:
Received 28 June 2013
Received in revised form
9 February 2014
Accepted 14 February 2014
Available online 13 March 2014

Keywords:
Ejector
Bypass
Annular cavity
CFD modeling
Performance

ABSTRACT

A bypass ejector geometry with an annular cavity in the nozzle wall was tested for various operating conditions to evaluate the entrainment performance. The results were compared with those of a conventional ejector. The data shows that the primary mass flow rate in the bypass ejector is always about 20% less than that in the conventional ejector. The results show that the bypass ejector is better than the conventional ejector at relatively high primary and secondary flow pressures with a maximum improvement in the entrainment performance of 31.5%. The bypass ejector has better entrainment performance in the critical mode. Since most ejectors operate in the critical mode, this ejector will have many applications requiring more entrainment.

© 2014 Elsevier Ltd. All rights reserved.

1. Introduction

The ejector is a simple fluid entrainment and circulation device which uses the venturi effect to convert the pressure energy of a motive primary fluid to kinetic energy to draw in and entrain a secondary fluid. The ejector is also known as a vacuum jet, jet pump or thermo-compressor for different applications, such as refrigeration systems [1], heat pumps [2], fuel cell systems [3], Kalina cycles [4] and Rankin Cycles [5].

The ejector performance is usually evaluated based on the entrainment ratio, which is defined as $\omega = m_s/m_p$. Therefore, increasing the secondary mass flow rate and decreasing the primary mass flow rate can both improve the ejector performance. The primary mass flow rate is determined by only the nozzle throat diameter and is independent of other ejector geometric parameters. The relation between the primary mass flow rate and the nozzle throat diameter has been well established in nozzle flow theory. Therefore, almost all existing ejector geometry optimization studies have focused on increasing the secondary mass flow rate.

The secondary mass flow rate is affected by various ejector geometric parameters, such as the primary nozzle throat diameter, the mixing chamber diameter, the primary NXP (nozzle exit position) and the converging angle of the mixing section (θ). Sun [6] analyzed the effect of the primary nozzle throat diameter and the mixing chamber diameter on ejector performance. Detailed design data was presented for the variable-geometry ejectors. Huang et al. [7] investigated 11 different ejectors and various operating conditions to show that the ejector performance is improved by increasing the diameter ratio between the mixing chamber and the nozzle throat. Aphornratana and Eames [8] studied the effect of the primary nozzle exit position on the system performance using an ejector with a movable primary nozzle. They showed that the nozzle exit position could be adjusted to maximize the system performance for operating conditions different from the design point. For the converge angle θ, ESDU (Engineering Sciences Data Unit) [9] recommended that the best design for the converging angle of the mixing section was about 10°. Zhu et al. [10] numerically studied 95 different ejector geometries to show that the optimum NXP is not only proportional to the mixing section throat diameter, but also increases as the primary flow pressure rises. The ejector performance is very sensitive to θ especially near the optimum working point. Liu et al. [11] investigated a variable geometry two-phase flow ejector to show that the motive nozzle efficiency decreases as the ejector throat area decreases.

In this study, a novel ejector configuration was designed to reduce the primary flow rate. The difference between this ejector and conventional ejectors is the primary nozzle. The primary nozzle of this ejector has an annular cavity in the nozzle wall which is connected to the primary nozzle inlet and the nozzle throat so as to create a bypass

* Corresponding author. Tel.: +86 10 62797038.
E-mail address: yinhai.zhu@mail.tsinghua.edu.cn (Y. Zhu).

http://dx.doi.org/10.1016/j.energy.2014.02.046
0360-5442/© 2014 Elsevier Ltd. All rights reserved.

Nomenclature

m	mass flow rate, g s^{-1}
P	pressure, MPa
T	temperature, K
ω	entrainment ratio, m_S/m_P
Subscripts	
P	primary flow
S	secondary flow
B	ejector exit
conv	conventional ejector
bypass	bypass ejector

for the primary flow. The mixing process of the bypass primary flow with the main part of the primary flow induces a large friction loss that reduces the mass flow rate. The bypass ejector has been tested for various operating conditions. The measured data is compared to data from a conventional ejector. CFD (computational fluid dynamics) models of the bypass ejector and the conventional ejector were also used to analyze the flow with comparisons with the experimental data. The working principle of the bypass ejector is discussed based on the detailed flow field and velocity distributions from the CFD model.

2. Experimental setup

2.1. Experimental system

Fig. 1 shows a schematic diagram of the experimental system using N_2 as the working fluid. The primary and secondary flows are supplied by eight N_2 tanks in parallel. The high-pressure N_2 (the primary flow) is accelerated to supersonic flow as it passes through the ejector nozzle to generate a low-pressure in the suction chamber capable of entraining the secondary flow. The motive primary flow and entrained the secondary flow then mix in the ejector. The mixed stream has shock waves in the diffuser when its kinetic energy is converted to pressure energy and then discharges directly to the environment.

The primary and the secondary flow pressures were controlled by two control values. The primary flow pressures, P_P, were varied from 0.3 to 0.55 MPa while the secondary flow pressures, P_S, were varied from 0.05 to 0.09 MPa. The back pressure at the ejector exit, P_B, was always close to the ambient pressure.

2.2. Experimental ejector

Fig. 2 shows schematics of the conventional ejector and the bypass ejector installed in the experimental rig which consisted of

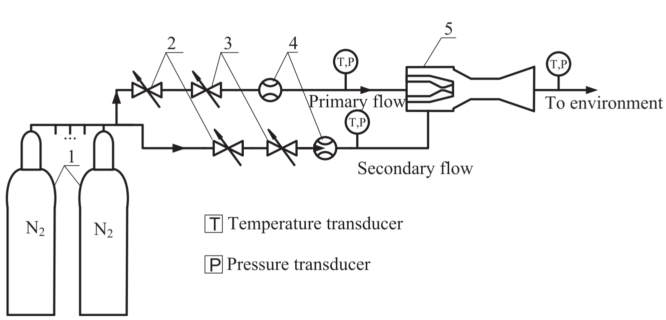

Fig. 1. Experimental rig. 1-High pressure N_2 tanks; 2-Pressure relief valves; 3-Terminal and control valves; 4-Mass flow meters; 5-Ejector.

the primary nozzle, the suction chamber, the mixing chamber and the diffuser. The suction chamber, the mixing chamber and the diffuser were connected by flanges. The primary nozzle was coupled by threads with the suction chamber so that the nozzles could be easily changed. The diameters of the primary and secondary inlets were both 16 mm. The diameter of the constant-area mixing chamber was 9.6 mm as shown in Fig. 2.

The difference between the conventional ejector and the bypass ejector is the nozzle. The primary nozzle in the conventional ejector was a convergent-divergent nozzle with a 3.6 mm nozzle throat diameter. The primary nozzle in the bypass ejector had an annular cavity inside the nozzle wall. Four small 1.5 mm diameter through holes connected the annular cavity to the nozzle inlet. The outlet of the annular cavity was connected to the nozzle throat. Therefore, the primary flow in the nozzle was divided into one flow path along the nozzle throat and another flow path which entered the annular cavity and then mixed with the first flow path in the nozzle throat. For ease of manufacture the bypass nozzle was designed as two parts as shown in Fig. 3.

2.3. Uncertainty analysis

1) Three pressure transducers with full scale errors of 0.5% (0–0.3 MPa; 0–0.3 MPa; 0–0.8 MPa).
2) Three PT100 platinum resistance temperature transducers with errors of 0.15 °C.
3) The mass flow rates of the primary flow and the secondary flow were measured by two coriolis-type mass flow rate meters (Model: Siemens MASS6000). According to the instructions, the accuracy of the mass flow meters was 0.1%. A detailed uncertainty analysis showed that the maximum uncertainty of the mass flow rate was 0.02 g/s.

3. CFD model

The numerical study used the commercial software ANSYS 13.0 FLUENT as the CFD solver. The flow in the ejector is governed by the compressible steady-state form of the fluid flow conservation equations. The governing equations of continuum, momentum and energy can be written in the cylindrical (x, r) coordinate system for axisymmetric flow as:

$$\frac{\partial}{\partial x}(\rho u)+\frac{\partial}{\partial r}(\rho v)+\frac{\rho v}{r}=0 \tag{1}$$

$$\frac{1}{r}\frac{\partial}{\partial x}(r\rho uu)+\frac{1}{r}\frac{\partial}{\partial r}(r\rho uv)=-\frac{\partial p}{\partial x}+\frac{1}{r}\frac{\partial}{\partial x}\left[r\mu\left(\frac{\partial u}{\partial x}-\frac{2}{3}(\nabla\cdot\vec{v})\right)\right]+\frac{1}{r}\frac{\partial}{\partial r}\left[r\mu\left(\frac{\partial u}{\partial r}+\frac{\partial v}{\partial x}\right)\right]+\rho g \tag{2}$$

$$\frac{1}{r}\frac{\partial}{\partial x}(r\rho uv)+\frac{1}{r}\frac{\partial}{\partial r}(r\rho vv)=-\frac{\partial p}{\partial r}+\frac{1}{r}\frac{\partial}{\partial r}\left[r\mu\left(2\frac{\partial v}{\partial r}-\frac{2}{3}(\nabla\cdot\vec{v})\right)\right]+\frac{1}{r}\frac{\partial}{\partial x}\left[r\mu\left(\frac{\partial u}{\partial r}+\frac{\partial v}{\partial x}\right)\right]-2\mu\frac{v}{r^2}+\frac{2}{3}\frac{\mu}{r}(\nabla\cdot\vec{v}) \tag{3}$$

$$\frac{\partial}{\partial x}(\rho uh)+\frac{\partial}{\partial r}(\rho vh)=\frac{\partial}{\partial x}\left(\lambda\frac{\partial T}{\partial x}\right)+\frac{\partial}{\partial r}\left(\lambda\frac{\partial T}{\partial r}\right)-\frac{\rho vh}{r}+\frac{\lambda}{r}\frac{\partial T}{\partial r}+S_h \tag{4}$$

where $(\nabla\cdot\vec{v})=\partial u/\partial x+\partial v/\partial r+v/r$ and S_h is the source term.

The ejector geometry was modeled in a 2D domain as shown in Fig. 4. The grid initially had about 40,000 elements which were

Download English Version:

https://daneshyari.com/en/article/8077972

Download Persian Version:

https://daneshyari.com/article/8077972

Daneshyari.com